Solar Si appendix

Sun · Si · downloadable appendix

Document	Solar Si appendix
Subject	Solar photospheric abundance appendix · Si
Author	Ryan Schmitt
Date	2026-11-09
Publisher	The Exoplanet Codex · exoplanetcodex.org
Version	feed v1.421
Source	science commit 078cf7dedfa9
Web	https://exoplanetcodex.org/systems/sol/elements/si/

Solar silicon: 7.573 ± 0.036

Asplund, Amarsi & Grevesse 2021: 7.51 ± 0.03 · this measurement +0.063 dex

Measured the way Asplund, Amarsi & Grevesse (2021) measure it: the Asplund et al. 2021 line set (Amarsi & Asplund 2017: nine Si I and one Si II line), 10 lines measured on one spectrum, each part weighted by its uncertainty.

Si I: 7.580 ± 0.037 · Kitt Peak (1984, molecfit) · VIS · Si I · Asplund et al. 2021 lines · 3D NLTE (Amarsi)

Si II: 7.522 ± 0.038 · Kitt Peak (1984, molecfit) · VIS · Si II · Asplund et al. 2021 lines · 1D LTE

Si I: 7.650 ± 0.051 · Kitt Peak (1984, molecfit) · red-optical · Si I · Asplund et al. 2021 lines · 3D NLTE (Amarsi)

Highlighted Products

VIS

7.580 ± 0.037

Si I · Asplund et al. 2021 lines · 3D NLTE (Amarsi) · Kitt Peak (1984, molecfit) · Reference Grade

red-optical

7.657 ± 0.050

Si I · Asplund et al. 2021 lines · 3D NLTE (Amarsi) · IAG FTS · Reference Grade

NIR

7.525 ± 0.041

Si I · Elgueta et al. 2026 lines · 1D NLTE (Amarsi) · Kitt Peak (1984, molecfit) · Reference Grade

H

7.327 ± 0.048

Si I · Elgueta et al. 2026 lines · 1D NLTE (Amarsi) · CRIRES+ H · Reference Grade

K

7.494 ± 0.078

Si I · Codex-graded lines · 1D NLTE (Amarsi) · CRIRES+ · Codex Grade

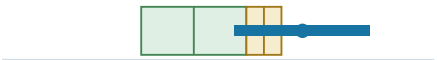
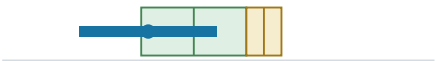
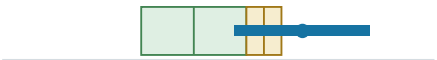
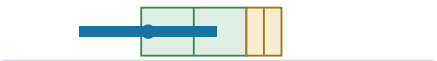
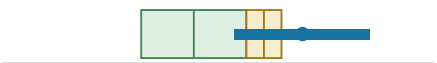
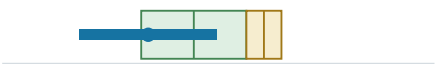
Line grades

Every product is measured on one of three grades of spectral lines and the grades are never mixed in one number.

Grade	What it means	This element
Reference Grade	lines from a published solar line set (Asplund et al. 2021 and similar), measured with the oscillator strengths the authors used	65 products -- Si I · Asplund et al. 2021 lines; Si I · Deshmukh et al. 2022 lines; Si I · Elgueta et al. 2026 lines; Si I · reference lines; Si II · Asplund et al. 2021 lines
Codex Grade	lines chosen by the Codex whose oscillator strength carries a published uncertainty (laboratory measurement, NIST accuracy class A-C, or the paper's own stated error), between 5% and 60% deep	39 products -- Si I · Codex-graded lines; Si II · Codex-graded lines
Deep Grade	the same oscillator-strength rule on lines deeper than 60% -- stronger lines, more sensitive to damping and the model atmosphere	none for the Sun: every line in this grade is excluded as saturated or an outlier (see Excluded lines)

Error-bar Forest Plot

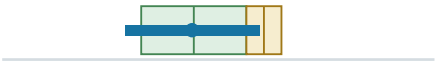
VIS — HARPS
A(Si) dex; axis 7.40–7.65

Si II · Asplund et al. 2021 lines · 1D LTE Reference Grade · 1 line		7.529 ±0.038
Si II · Codex-graded lines · 1D LTE Codex Grade · 3 lines		7.502 ±0.039
Si I · Asplund et al. 2021 lines · 1D LTE Reference Grade · 7 lines		7.511 ±0.039
Si I · Asplund et al. 2021 lines · 3D NLTE (Amarsi) Reference Grade · 7 lines		7.572 ±0.039
Si I · Asplund et al. 2021 lines · 1D NLTE (Amarsi) Reference Grade · 7 lines		7.484 ±0.039
Si I · Codex-graded lines · 1D LTE Codex Grade · 7 lines		7.511 ±0.039
Si I · Codex-graded lines · 3D NLTE (Amarsi) Codex Grade · 7 lines		7.572 ±0.039
Si I · Codex-graded lines · 1D NLTE (Amarsi) Codex Grade · 7 lines		7.484 ±0.039
Si I · reference lines · 1D LTE Reference Grade · 7 lines		7.511 ±0.039
Si I · reference lines · 3D NLTE (Amarsi) Reference Grade · 7 lines		7.572 ±0.039
Si I · reference lines · 1D NLTE (Amarsi) Reference Grade · 7 lines		7.484 ±0.039

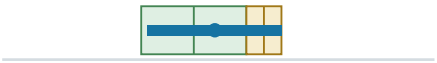
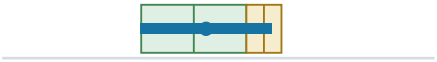
VIS — Kitt Peak (Kurucz 2005)
A(Si) dex; axis 7.40–7.65

Si II · Asplund et al. 2021 lines · 1D LTE Reference Grade · 1 line		7.528 ±0.038

VIS — Kitt Peak (Kurucz 2005)
A(Si) dex; axis 7.40–7.65

Si II · Codex-graded lines · 1D LTE Codex Grade · 3 lines		7.528 ±0.075
Si I · Asplund et al. 2021 lines · 1D LTE Reference Grade · 7 lines		7.509 ±0.038
Si I · Asplund et al. 2021 lines · 3D NLTE (Amarsi) Reference Grade · 7 lines		7.572 ±0.038
Si I · Asplund et al. 2021 lines · 1D NLTE (Amarsi) Reference Grade · 7 lines		7.482 ±0.039
Si I · Codex-graded lines · 1D LTE Codex Grade · 7 lines		7.509 ±0.038
Si I · Codex-graded lines · 3D NLTE (Amarsi) Codex Grade · 7 lines		7.572 ±0.038
Si I · Codex-graded lines · 1D NLTE (Amarsi) Codex Grade · 7 lines		7.482 ±0.039
Si I · reference lines · 1D LTE Reference Grade · 7 lines		7.509 ±0.038
Si I · reference lines · 3D NLTE (Amarsi) Reference Grade · 7 lines		7.572 ±0.038
Si I · reference lines · 1D NLTE (Amarsi) Reference Grade · 7 lines		7.482 ±0.039

VIS — Kitt Peak (1984, molecfit)
A(Si) dex; axis 7.40–7.65

Si II · Asplund et al. 2021 lines · 1D LTE Reference Grade · 1 line		7.522 ±0.038
Si II · Codex-graded lines · 1D LTE Codex Grade · 3 lines		7.522 ±0.091
Si I · Asplund et al. 2021 lines · 1D LTE Reference Grade · 7 lines		7.517 ±0.038
Si I · Asplund et al. 2021 lines · 3D NLTE (Amarsi) Reference Grade · 7 lines		7.580 ±0.037
Si I · Asplund et al. 2021 lines · 1D NLTE (Amarsi) Reference Grade · 7 lines		7.490 ±0.038
Si I · Codex-graded lines · 1D LTE Codex Grade · 7 lines		7.517 ±0.038
Si I · Codex-graded lines · 3D NLTE (Amarsi) Codex Grade · 7 lines		7.580 ±0.037
Si I · Codex-graded lines · 1D NLTE (Amarsi) Codex Grade · 7 lines		7.490 ±0.038

VIS — Kitt Peak (1984, molecfit)
A(Si) dex; axis 7.40–7.65

Si I · reference lines · 1D LTE Reference Grade · 7 lines		7.517 ±0.038
Si I · reference lines · 3D NLTE (Amarsi) Reference Grade · 7 lines		7.580 ±0.037
Si I · reference lines · 1D NLTE (Amarsi) Reference Grade · 7 lines		7.490 ±0.038

VIS axis: 7.40 · 7.46 · 7.52 · 7.59 · 7.65 A(Si) dex

red-optical — IAG FTS
A(Si) dex; axis 7.45–7.74

Si I · Asplund et al. 2021 lines · 1D LTE Reference Grade · 2 lines		7.595 ±0.044
Si I · Asplund et al. 2021 lines · 3D NLTE (Amarsi) Reference Grade · 2 lines		7.657 ±0.050
Si I · Asplund et al. 2021 lines · 1D NLTE (Amarsi) Reference Grade · 2 lines		7.576 ±0.043
Si I · Codex-graded lines · 1D LTE Codex Grade · 87 lines		7.537 ±0.049
Si I · Codex-graded lines · 3D NLTE (Amarsi) Codex Grade · 2 lines		7.657 ±0.050
Si I · Codex-graded lines · 1D NLTE (Amarsi) Codex Grade · 83 lines		7.527 ±0.050
Si I · reference lines · 1D LTE Reference Grade · 2 lines		7.595 ±0.044
Si I · reference lines · 3D NLTE (Amarsi) Reference Grade · 2 lines		7.657 ±0.050
Si I · reference lines · 1D NLTE (Amarsi) Reference Grade · 2 lines		7.576 ±0.043

red-optical — Kitt Peak (Kurucz 2005)
A(Si) dex; axis 7.45–7.74

Si I · Asplund et al. 2021 lines · 1D LTE Reference Grade · 2 lines		7.582 ±0.045
Si I · Asplund et al. 2021 lines · 3D NLTE (Amarsi) Reference Grade · 2 lines		7.645 ±0.051
Si I · Asplund et al. 2021 lines · 1D NLTE (Amarsi) Reference Grade · 2 lines		7.564 ±0.043
Si I · Codex-graded lines · 1D LTE Codex Grade · 86 lines		7.549 ±0.049

red-optical — Kitt Peak (Kurucz 2005)
A(Si) dex; axis 7.45–7.74

Si I · Codex-graded lines · 3D NLTE (Amarsi) Codex Grade · 2 lines		7.645 ±0.051
Si I · Codex-graded lines · 1D NLTE (Amarsi) Codex Grade · 83 lines		7.538 ±0.049
Si I · reference lines · 1D LTE Reference Grade · 2 lines		7.582 ±0.045
Si I · reference lines · 3D NLTE (Amarsi) Reference Grade · 2 lines		7.645 ±0.051
Si I · reference lines · 1D NLTE (Amarsi) Reference Grade · 2 lines		7.564 ±0.043

red-optical — Kitt Peak (1984, molecfit)
A(Si) dex; axis 7.45–7.74

Si I · Asplund et al. 2021 lines · 1D LTE Reference Grade · 2 lines		7.587 ±0.045
Si I · Asplund et al. 2021 lines · 3D NLTE (Amarsi) Reference Grade · 2 lines		7.650 ±0.051
Si I · Asplund et al. 2021 lines · 1D NLTE (Amarsi) Reference Grade · 2 lines		7.569 ±0.044
Si I · Codex-graded lines · 1D LTE Codex Grade · 85 lines		7.553 ±0.048
Si I · Codex-graded lines · 3D NLTE (Amarsi) Codex Grade · 2 lines		7.650 ±0.051
Si I · Codex-graded lines · 1D NLTE (Amarsi) Codex Grade · 82 lines		7.534 ±0.048
Si I · reference lines · 1D LTE Reference Grade · 2 lines		7.587 ±0.045
Si I · reference lines · 3D NLTE (Amarsi) Reference Grade · 2 lines		7.650 ±0.051
Si I · reference lines · 1D NLTE (Amarsi) Reference Grade · 2 lines		7.569 ±0.044

red-optical axis: 7.45 · 7.52 · 7.59 · 7.66 · 7.74 A(Si) dex

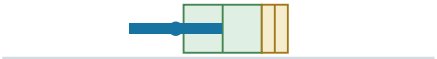
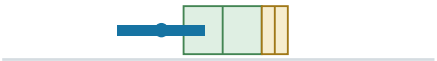
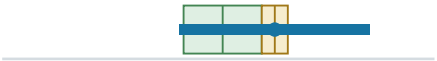
NIR — CRIRES+ J
A(Si) dex; axis 7.34–7.67

Si I · Deshmukh et al. 2022 lines · 1D LTE Reference Grade · 2 lines		7.516 ±0.032
Si I · Deshmukh et al. 2022 lines · 1D NLTE (Amarsi) Reference Grade · 2 lines		7.490 ±0.032

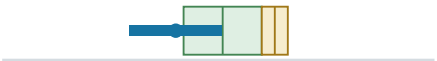
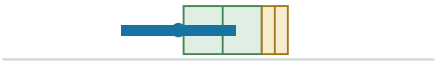
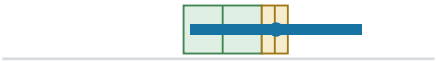
NIR — CRIRES+ J
A(Si) dex; axis 7.34–7.67

Si I · Elgueta et al. 2026 lines · 1D LTE Reference Grade · 9 lines		7.517 ±0.044
Si I · Codex-graded lines · 1D LTE Codex Grade · 27 lines		7.524 ±0.055
Si I · Codex-graded lines · 1D NLTE (Amarsi) Codex Grade · 27 lines		7.504 ±0.055
Si I · reference lines · 1D LTE Reference Grade · 2 lines		7.516 ±0.032
Si I · reference lines · 1D NLTE (Amarsi) Reference Grade · 2 lines		7.490 ±0.032

NIR — CRIRES+ Y
A(Si) dex; axis 7.34–7.67

Si I · Deshmukh et al. 2022 lines · 1D LTE Reference Grade · 1 line		7.474 ±0.035
Si I · Deshmukh et al. 2022 lines · 1D NLTE (Amarsi) Reference Grade · 1 line		7.434 ±0.035
Si I · Elgueta et al. 2026 lines · 1D LTE Reference Grade · 2 lines		7.463 ±0.034
Si I · Elgueta et al. 2026 lines · 1D NLTE (Amarsi) Reference Grade · 2 lines		7.436 ±0.032
Si I · Codex-graded lines · 1D LTE Codex Grade · 4 lines		7.550 ±0.073
Si I · Codex-graded lines · 1D NLTE (Amarsi) Codex Grade · 4 lines		7.528 ±0.077

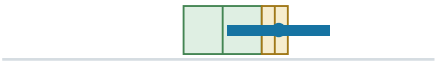
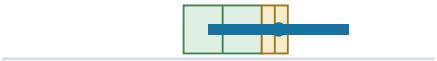
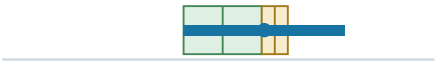
NIR — CRIRES+ Y (full arm)
A(Si) dex; axis 7.34–7.67

Si I · Deshmukh et al. 2022 lines · 1D LTE Reference Grade · 1 line		7.474 ±0.035
Si I · Deshmukh et al. 2022 lines · 1D NLTE (Amarsi) Reference Grade · 1 line		7.434 ±0.035
Si I · Elgueta et al. 2026 lines · 1D LTE Reference Grade · 5 lines		7.476 ±0.044
Si I · Codex-graded lines · 1D LTE Codex Grade · 8 lines		7.579 ±0.064
Si I · Codex-graded lines · 1D NLTE (Amarsi) Codex Grade · 8 lines		7.551 ±0.066

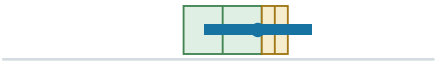
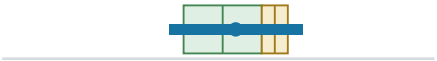
NIR — IAG FTS
A(Si) dex; axis 7.34–7.67

Si I · Elgueta et al. 2026 lines · 1D LTE Reference Grade · 1 line		7.550 ±0.041
Si I · Elgueta et al. 2026 lines · 1D NLTE (Amarsi) Reference Grade · 1 line		7.538 ±0.041
Si I · Codex-graded lines · 1D LTE Codex Grade · 13 lines		7.504 ±0.096
Si I · Codex-graded lines · 1D NLTE (Amarsi) Codex Grade · 9 lines		7.496 ±0.125

NIR — Kitt Peak (Kurucz 2005)
A(Si) dex; axis 7.34–7.67

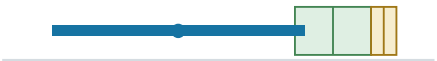
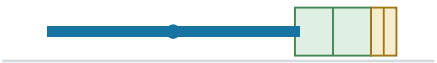
Si I · Elgueta et al. 2026 lines · 1D LTE Reference Grade · 1 line		7.553 ±0.039
Si I · Elgueta et al. 2026 lines · 1D NLTE (Amarsi) Reference Grade · 1 line		7.541 ±0.039
Si I · Codex-graded lines · 1D LTE Codex Grade · 13 lines		7.553 ±0.054
Si I · Codex-graded lines · 1D NLTE (Amarsi) Codex Grade · 9 lines		7.542 ±0.062

NIR — Kitt Peak (1984, molecfit)
A(Si) dex; axis 7.34–7.67

Si I · Deshmukh et al. 2022 lines · 1D LTE Reference Grade · 3 lines		7.580 ±0.045
Si I · Deshmukh et al. 2022 lines · 1D NLTE (Amarsi) Reference Grade · 3 lines		7.551 ±0.048
Si I · Elgueta et al. 2026 lines · 1D LTE Reference Grade · 15 lines		7.537 ±0.041
Si I · Elgueta et al. 2026 lines · 1D NLTE (Amarsi) Reference Grade · 15 lines		7.525 ±0.041
Si I · Codex-graded lines · 1D LTE Codex Grade · 48 lines		7.520 ±0.051
Si I · Codex-graded lines · 1D NLTE (Amarsi) Codex Grade · 44 lines		7.510 ±0.047
Si I · reference lines · 1D LTE Reference Grade · 2 lines		7.588 ±0.033
Si I · reference lines · 1D NLTE (Amarsi) Reference Grade · 2 lines		7.562 ±0.034

NIR axis: 7.34 · 7.42 · 7.51 · 7.59 · 7.67 A(Si) dex

H — CRIRES+ H
A(Si) dex; axis 7.25–7.59

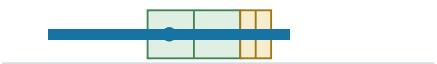
Si I · Elgueta et al. 2026 lines · 1D LTE Reference Grade · 3 lines		7.365 ±0.050
Si I · Elgueta et al. 2026 lines · 1D NLTE (Amarsi) Reference Grade · 3 lines		7.327 ±0.048
Si I · Codex-graded lines · 1D LTE Codex Grade · 27 lines		7.388 ±0.099
Si I · Codex-graded lines · 1D NLTE (Amarsi) Codex Grade · 27 lines		7.384 ±0.099

H — CRIRES+ H (full arm, telluric-corrected)
A(Si) dex; axis 7.25–7.59

Si I · Elgueta et al. 2026 lines · 1D LTE Reference Grade · 3 lines		7.425 ±0.063
Si I · Elgueta et al. 2026 lines · 1D NLTE (Amarsi) Reference Grade · 3 lines		7.387 ±0.057
Si I · Codex-graded lines · 1D LTE Codex Grade · 44 lines		7.426 ±0.072
Si I · Codex-graded lines · 1D NLTE (Amarsi) Codex Grade · 44 lines		7.420 ±0.072

H axis: 7.25 · 7.33 · 7.42 · 7.50 · 7.59 A(Si) dex

K — CRIRES+
A(Si) dex; axis 7.39–7.67

Si I · Codex-graded lines · 1D LTE Codex Grade · 11 lines		7.559 ±0.077
Si I · Codex-graded lines · 1D NLTE (Amarsi) Codex Grade · 11 lines		7.494 ±0.078

K axis: 7.39 · 7.46 · 7.53 · 7.60 · 7.67 A(Si) dex

How to read this forest. Each row is one independent product, preserving its band, holding, engine, indicator and line set. Engines and indicator families are never averaged. Each bar is the uncertainty as Asplund et al. 2021 quote it: line-to-line scatter, the 3D-model term and the NLTE term (at least 0.03 dex). For a molecule the NLTE term is replaced by its dependence on the other element, and the 3D term comes from the 3D-to-1D difference Amarsi et al. 2021 publish for the same band. Atomic-data and observational terms are not in the bar, as in Asplund; they stay in the full error budget attached to the row. Grades describe the supplied line-pool provenance, not engine quality; evaluated theoretical CNO oscillator strengths are not relabelled as laboratory evidence. Quarantined, failed and unconstrained fits have no abundance mark. Experimental products remain explicitly not adopted. Literature references provide context, never tuning targets.

How this was measured

Every silicon value on this page comes from fitting synthetic spectra to the observed solar spectrum, line by line or band by band, with the silicon abundance as the free parameter. The synthesis includes the atomic lines and the molecular opacity in every window, so blended absorption is modelled rather than attributed to the line being measured. The continuum is placed locally around every line by comparing the observation with the synthesis on its own highest pixels, and ground-based spectra are telluric-corrected across their full range.

Each indicator is measured independently on each solar spectrum and reported separately; nothing is averaged across indicators or instruments. Where a 3D or NLTE correction is published for the lines, it is applied as its own product (1D-LTE, 1D-NLTE and 3D-NLTE are separate rows). Every value carries a full uncertainty budget: fit, line strengths, microturbulence, continuum, fit window, model atmosphere, telluric residual, and the spread between spectra, each measured by refitting with that one input changed. The headline at the top is the Asplund-grade product: a published line set, the most complete treatment, then the most lines.

Band	VIS
What was measured	Si I · Codex-graded lines; Si II · Codex-graded lines
Solar spectra	HARPS, Kitt Peak (1984, molecfit), Kitt Peak (Kurucz 2005)
Treatments	1D-LTE, 1D-NLTE, 3D-NLTE
Lines	3–7
Result A(Si)	7.572–7.580 (3D-NLTE)
Largest uncertainty terms (dex)	line strengths (gf) 0.05, NLTE / 3D correction 0.03

Band	VIS
What was measured	Si I · reference lines
Solar spectra	HARPS, Kitt Peak (1984, molecfit), Kitt Peak (Kurucz 2005)
Treatments	1D-LTE, 1D-NLTE, 3D-NLTE
Lines	7
Result A(Si)	7.572–7.580 (3D-NLTE)
Largest uncertainty terms (dex)	line strengths (gf) 0.05, NLTE / 3D correction 0.03

Band	VIS
What was measured	Si I · Asplund et al. 2021 lines; Si II · Asplund et al. 2021 lines
Solar spectra	HARPS, Kitt Peak (1984, molecfit), Kitt Peak (Kurucz 2005)
Treatments	1D-LTE, 1D-NLTE, 3D-NLTE
Lines	1–7
Result A(Si)	7.572–7.580 (3D-NLTE)
Largest uncertainty terms (dex)	line strengths (gf) 0.05, NLTE / 3D correction 0.03

Band	red-optical
What was measured	Si I · Codex-graded lines
Solar spectra	IAG FTS, Kitt Peak (1984, molecfit), Kitt Peak (Kurucz 2005)
Treatments	1D-LTE, 1D-NLTE, 3D-NLTE
Lines	2–87

Band	red-optical
What was measured	Si I · Codex-graded lines
Result A(Si)	7.645–7.657 (3D-NLTE)
Largest uncertainty terms (dex)	line strengths (gf) 0.11, fit / line-to-line scatter 0.04

Band	red-optical
What was measured	Si I · reference lines
Solar spectra	IAG FTS, Kitt Peak (1984, molecfit), Kitt Peak (Kurucz 2005)
Treatments	1D-LTE, 1D-NLTE, 3D-NLTE
Lines	2
Result A(Si)	7.645–7.657 (3D-NLTE)
Largest uncertainty terms (dex)	line strengths (gf) 0.11, fit / line-to-line scatter 0.04

Band	red-optical
What was measured	Si I · Asplund et al. 2021 lines
Solar spectra	IAG FTS, Kitt Peak (1984, molecfit), Kitt Peak (Kurucz 2005)
Treatments	1D-LTE, 1D-NLTE, 3D-NLTE
Lines	2
Result A(Si)	7.645–7.657 (3D-NLTE)
Largest uncertainty terms (dex)	line strengths (gf) 0.11, fit / line-to-line scatter 0.04

Band	NIR
What was measured	Si I · Codex-graded lines
Solar spectra	CRIRES+ J, CRIRES+ Y, CRIRES+ Y (full arm), IAG FTS, Kitt Peak (1984, molecfit), Kitt Peak (Kurucz 2005)
Treatments	1D-LTE, 1D-NLTE
Lines	4–48
Result A(Si)	7.496–7.551 (1D-NLTE)
Largest uncertainty terms (dex)	line strengths (gf) 0.04, fit / line-to-line scatter 0.03

Band	NIR
What was measured	Si I · reference lines
Solar spectra	CRIRES+ J, Kitt Peak (1984, molecfit)
Treatments	1D-LTE, 1D-NLTE
Lines	2
Result A(Si)	7.490–7.562 (1D-NLTE)
Largest uncertainty terms (dex)	line strengths (gf) 0.07, NLTE / 3D correction 0.03

Band	NIR
What was measured	Si I · Deshmukh et al. 2022 lines
Solar spectra	CRIRES+ J, CRIRES+ Y, CRIRES+ Y (full arm), Kitt Peak (1984, molecfit)

Band	NIR
What was measured	Si I · Deshmukh et al. 2022 lines
Treatments	1D-LTE, 1D-NLTE
Lines	1–3
Result A(Si)	7.434–7.551 (1D-NLTE)
Largest uncertainty terms (dex)	line strengths (gf) 0.06, fit / line-to-line scatter 0.04

Band	NIR
What was measured	Si I · Elgueta et al. 2026 lines
Solar spectra	CRIRES+ J, CRIRES+ Y, CRIRES+ Y (full arm), IAG FTS, Kitt Peak (1984, molecfit), Kitt Peak (Kurucz 2005)
Treatments	1D-LTE, 1D-NLTE
Lines	1–15
Result A(Si)	7.436–7.541 (1D-NLTE)
Largest uncertainty terms (dex)	line strengths (gf) 0.04, NLTE / 3D correction 0.03

Band	H
What was measured	Si I · Codex-graded lines
Solar spectra	CRIRES+ H, CRIRES+ H (full arm, telluric-corrected)
Treatments	1D-LTE, 1D-NLTE
Lines	27–44
Result A(Si)	7.384–7.420 (1D-NLTE)
Largest uncertainty terms (dex)	fit / line-to-line scatter 0.06, line strengths (gf) 0.04

Band	H
What was measured	Si I · Elgueta et al. 2026 lines
Solar spectra	CRIRES+ H, CRIRES+ H (full arm, telluric-corrected)
Treatments	1D-LTE, 1D-NLTE
Lines	3
Result A(Si)	7.327–7.387 (1D-NLTE)
Largest uncertainty terms (dex)	line strengths (gf) 0.05, fit / line-to-line scatter 0.04

Band	K
What was measured	Si I · Codex-graded lines
Solar spectra	CRIRES+
Treatments	1D-LTE, 1D-NLTE
Lines	11
Result A(Si)	7.494 (1D-NLTE)
Largest uncertainty terms (dex)	fit / line-to-line scatter 0.07, line strengths (gf) 0.04

Excluded lines

These lines are left out of the Sun's measurement. They stay in the line lists: a cooler or more evolved star may measure them well. Blended lines are not excluded -- the spectrum synthesis models the blend. 59 lines.

Abundance outlier: disagrees with the other lines well beyond its error, and no solar analysis in the literature uses it.

Not measurable: the line falls in a data gap or a saturated telluric band.

Saturated: on the flat part of the curve of growth, so the line barely responds to the abundance (reduced width log W/λ above -4.9).

Species	Wavelength (Å, air)	Why it is excluded
Si II	3203.872	saturated (log W/λ = -4.18)
Si II	3210.028	saturated (log W/λ = -3.98)
Si II	3339.818	saturated (log W/λ = -4.04)
Si II	3856.017	saturated (log W/λ = -3.90)
Si II	3862.595	saturated (log W/λ = -4.15)
Si I	3905.523	saturated (log W/λ = -3.85)
Si I	4102.936	saturated (log W/λ = -4.10)
Si I	5948.541	saturated (log W/λ = -4.79)
Si I	7918.383	saturated (log W/λ = -4.88)
Si I	7932.348	saturated (log W/λ = -4.81)
Si I	7944.001	saturated (log W/λ = -4.75)
Si I	8543.151	saturated (log W/λ = -4.23)
Si I	8648.465	saturated (log W/λ = -4.72)
Si I	8661.177	saturated (log W/λ = -4.27)
Si I	8728.010	saturated (log W/λ = -4.89)
Si I	8742.446	saturated (log W/λ = -4.90)
Si I	8752.007	saturated (log W/λ = -4.79)
Si I	8790.389	saturated (log W/λ = -4.82)
Si I	9021.590	saturated (log W/λ = -4.88)
Si I	9413.500	saturated (log W/λ = -4.56)
Si I	9887.047	abundance outlier
Si I	10313.197	abundance outlier
Si I	10371.263	saturated (log W/λ = -4.73)
Si I	10585.141	saturated (log W/λ = -4.46)
Si I	10603.425	saturated (log W/λ = -4.57)
Si I	10627.648	saturated (log W/λ = -4.85)
Si I	10660.973	saturated (log W/λ = -4.53)
Si I	10689.716	saturated (log W/λ = -4.70)
Si I	10694.251	saturated (log W/λ = -4.66)
Si I	10727.406	saturated (log W/λ = -4.62)
Si I	10749.378	saturated (log W/λ = -4.54)
Si I	10786.849	saturated (log W/λ = -4.59)
Si I	10827.088	saturated (log W/λ = -4.40)
Si I	10843.858	saturated (log W/λ = -4.73)

Species	Wavelength (Å, air)	Why it is excluded
Si I	10868.790	saturated (log W/λ = -4.49)
Si I	10869.536	saturated (log W/λ = -4.34)
Si I	10885.333	saturated (log W/λ = -4.84)
Si I	10979.308	saturated (log W/λ = -4.62)
Si I	10982.058	saturated (log W/λ = -4.90)
Si I	11017.966	saturated (log W/λ = -4.68)
Si I	11187.588	saturated (log W/λ = -4.89)
Si I	11289.829	saturated (log W/λ = -4.86)
Si I	11611.060	saturated (log W/λ = -4.60)
Si I	11984.198	saturated (log W/λ = -4.46)
Si I	11991.568	saturated (log W/λ = -4.51)
Si I	12031.504	saturated (log W/λ = -4.38)
Si I	12103.534	saturated (log W/λ = -4.59)
Si I	12189.241	abundance outlier
Si I	12270.692	saturated (log W/λ = -4.62)
Si I	15077.332	saturated (log W/λ = -4.67)
Si I	15557.778	saturated (log W/λ = -4.88)
Si I	15888.409	saturated (log W/λ = -4.39)
Si I	15960.063	saturated (log W/λ = -4.53)
Si I	16060.009	saturated (log W/λ = -4.64)
Si I	16163.691	saturated (log W/λ = -4.78)
Si I	16380.176	saturated (log W/λ = -4.72)
Si I	16381.534	saturated (log W/λ = -4.54)
Si I	16434.927	not measurable
Si I	17466.879	saturated (log W/λ = -4.45)

Solar silicon context

Silicon is traced by Si I lines from the blue to the H band and by the single Si II 6371 Å line. The optical lines are Asplund et al. 2021's set (Amarsi & Asplund 2017) with the gf the authors used; the infrared lines are the published sets of Deshmukh et al. 2022 and Elgueta et al. 2026 on Pehlivan Rhodin et al. 2024 oscillator strengths. Each set, spectrum and treatment remains a separate product.

Published line sets · gf uncertainty model · Methodology

Download the evidence

Download PDF — Solar Si appendix

Source feed — includes quarantined fit outputs, not adopted abundances

Complete product visibility audit

Shared website/PDF report

Reproducibility manifest

Complete references and product-to-source bindings

Reproducibility

Generated from the pinned science snapshot. Source commit 078cf7dedfa961452c8bd9af43c4bf83c5463fdf
Feed Si.json v1.421 · updated 2026-11-09T10:06:41Z
Generated 2026-11-09T08:19:44-07:00 (source commit timestamp)
Feed SHA-256 18b210c58bf693b5755985de9cc6fdce611b4b95a0eb8e0093ff45d0326b19df
Generator scripts/generate_cno_publication.py v1.0.0

Pinned scientific source

References / Data & Model Sources

Sources are separated by their role. Registered grid lineage and quarantined diagnostics do not imply an adopted abundance or an applied correction.

See the source notes for the distinction between reference lineage and the treatment actually recorded in each feed entry.

Science and provenance source notes

Solar abundance and indicator analyses. Solar Si comparison literature; not an adopted Codex abundance. Sources: [1], [2].

Solar abundance and indicator analyses. Published line set SI_AGSS21 (the line selection). Sources: [3].

Atomic data and gf authorities. Si II oscillator strengths of this pool, as the product's own uncertainty budget records them (with their lineage). Sources: [3], [4], [5].

Model and grid sources. Feed treatment: 1D-LTE synthesis (Turbospectrum); no NLTE/3D correction claimed. Sources: [6].

Solar abundance and indicator analyses. Published line set SI_ELGUETA2026 (the line selection). Sources: [8].

Atomic data and gf authorities. Si I oscillator strengths of this pool, as the product's own uncertainty budget records them (with their lineage). Sources: [9].

Model and grid sources. Feed treatment: 1D NLTE, per-line correction from the Amarsi 2020 GALAH departure grid via PySME (data/nlte_grids/Si_Amarsi2020_PySME.csv). Sources: [10].

Solar abundance and indicator analyses. Published line set SI_DESHMUKH2022 (the line selection). Sources: [11].

Model and grid sources. Cited solar abundance differences from the published model columns, applied additively to our LTE fits; not a new in-transfer 3D calculation. Baseline atmosphere: A_marcs_lte Sources: [3].

Product-to-source index

VIS · HARPS · Si II · Asplund et al. 2021 lines · 1D LTE · [1], [2], [3], [4], [5], [6] Si-products-18313ebf6e74

VIS · HARPS · Si II · Codex-graded lines · 1D LTE · [1], [2], [7], [3], [4], [5], [6] Si-products-a600a1f3ca00

VIS · Kitt Peak (Kurucz 2005) · Si II · Asplund et al. 2021 lines · 1D LTE · [1], [2], [3], [4], [5], [6] Si-products-7b250bcdf59f

VIS · Kitt Peak (Kurucz 2005) · Si II · Codex-graded lines · 1D LTE · [1], [2], [7], [3], [4], [5], [6] Si-products-8d7dbfa460a5

VIS · Kitt Peak (1984, molecfit) · Si II · Asplund et al. 2021 lines · 1D LTE · [1], [2], [3], [4], [5], [6] Si-products-7f5a70dae4b6

VIS · Kitt Peak (1984, molecfit) · Si II · Codex-graded lines · 1D LTE · [1], [2], [7], [3], [4], [5], [6] Si-products-d48b7d00757a

H · CRIRES+ H · Si I · Elgueta et al. 2026 lines · 1D LTE · [1], [2], [8], [9], [6] Si-products-ae368e68c20f

H · CRIRES+ H · Si I · Elgueta et al. 2026 lines · 1D NLTE (Amarsi) · [1], [2], [8], [9], [10] Si-products-dce72b125a33

H · CRIRES+ H · Si I · Codex-graded lines · 1D LTE · [1], [2], [9], [6] Si-products-1d967903fd3d

H · CRIRES+ H · Si I · Codex-graded lines · 1D NLTE (Amarsi) · [1], [2], [9], [10] Si-products-dc9ebf2d12b4

H · CRIRES+ H (full arm, telluric-corrected) · Si I · Elgueta et al. 2026 lines · 1D LTE · [1], [2], [8], [9], [6] Si-products-e636e6942aaf

H · CRIRES+ H (full arm, telluric-corrected) · Si I · Elgueta et al. 2026 lines · 1D NLTE (Amarsi) · [1], [2], [8], [9], [10] Si-products-50ccbe6c093c

H · CRIRES+ H (full arm, telluric-corrected) · Si I · Codex-graded lines · 1D LTE · [1], [2], [9], [6] Si-products-83868b6649f2

H · CRIRES+ H (full arm, telluric-corrected) · Si I · Codex-graded lines · 1D NLTE (Amarsi) · [1], [2], [9], [10] Si-products-4e3d20d18453

K · CRIRES+ · Si I · Codex-graded lines · 1D LTE · [1], [2], [9], [7], [6] Si-products-e5909f30041c

K · CRIRES+ · Si I · Codex-graded lines · 1D NLTE (Amarsi) · [1], [2], [9], [7], [10] Si-products-b3ab69cd715a

NIR · CRIRES+ J · Si I · Deshmukh et al. 2022 lines · 1D LTE · [1], [2], [11], [9], [6] Si-products-2c4a49bae319

NIR · CRIRES+ J · Si I · Deshmukh et al. 2022 lines · 1D NLTE (Amarsi) · [1], [2], [11], [9], [10] Si-products-3fcf18c258ba

NIR · CRIRES+ J · Si I · Elgueta et al. 2026 lines · 1D LTE · [1], [2], [8], [9], [6] Si-products-b3c6ecb92cd3

NIR · CRIRES+ J · Si I · Codex-graded lines · 1D LTE · [1], [2], [9], [6] Si-products-ad080159c97e

NIR · CRIRES+ J · Si I · Codex-graded lines · 1D NLTE (Amarsi) · [1], [2], [9], [10] Si-products-8f790841b86a

NIR · CRIRES+ J · Si I · reference lines · 1D LTE · [1], [2], [9], [6] Si-products-fbf87a47d2fb

NIR · CRIRES+ J · Si I · reference lines · 1D NLTE (Amarsi) · [1], [2], [9], [10] Si-products-c1bcbd9b9ec0

NIR · CRIRES+ Y · Si I · Deshmukh et al. 2022 lines · 1D LTE · [1], [2], [11], [9], [6] Si-products-153e9d83ac68

NIR · CRIRES+ Y · Si I · Deshmukh et al. 2022 lines · 1D NLTE (Amarsi) · [1], [2], [11], [9], [10] Si-products-3c32a05acba0

NIR · CRIRES+ Y · Si I · Elgueta et al. 2026 lines · 1D LTE · [1], [2], [8], [9], [6] Si-products-d6010398e58a

NIR · CRIRES+ Y · Si I · Elgueta et al. 2026 lines · 1D NLTE (Amarsi) · [1], [2], [8], [9], [10] Si-products-aa9e3a7485c1

NIR · CRIRES+ Y · Si I · Codex-graded lines · 1D LTE · [1], [2], [9], [6] Si-products-07fb3d10f039

NIR · CRIRES+ Y · Si I · Codex-graded lines · 1D NLTE (Amarsi) · [1], [2], [9], [10] Si-products-1d17eaa1fe36

NIR · CRIRES+ Y (full arm) · Si I · Deshmukh et al. 2022 lines · 1D LTE · [1], [2], [11], [9], [6] Si-products-fff5b3b19703

NIR · CRIRES+ Y (full arm) · Si I · Deshmukh et al. 2022 lines · 1D NLTE (Amarsi) · [1], [2], [11], [9], [10] Si-products-bb2f4678ac4a

NIR · CRIRES+ Y (full arm) · Si I · Elgueta et al. 2026 lines · 1D LTE · [1], [2], [8], [9], [6] Si-products-1254152a3e1d

NIR · CRIRES+ Y (full arm) · Si I · Codex-graded lines · 1D LTE · [1], [2], [9], [6] Si-products-fc0c7f3fdd87

NIR · CRIRES+ Y (full arm) · Si I · Codex-graded lines · 1D NLTE (Amarsi) · [1], [2], [9], [10] Si-products-dbc6e56c6748

NIR · IAG FTS · Si I · Elgueta et al. 2026 lines · 1D LTE · [1], [2], [8], [9], [6] Si-products-b5727388eb1e

NIR · IAG FTS · Si I · Elgueta et al. 2026 lines · 1D NLTE (Amarsi) · [1], [2], [8], [9], [10] Si-products-8f63065469b7

NIR · IAG FTS · Si I · Codex-graded lines · 1D LTE · [1], [2], [9], [6] Si-products-ed6a2068925c

NIR · IAG FTS · Si I · Codex-graded lines · 1D NLTE (Amarsi) · [1], [2], [9], [10] Si-products-771b4c0aca06

NIR · Kitt Peak (Kurucz 2005) · Si I · Elgueta et al. 2026 lines · 1D LTE · [1], [2], [8], [9], [6] Si-products-0c0ff2a52c28

NIR · Kitt Peak (Kurucz 2005) · Si I · Elgueta et al. 2026 lines · 1D NLTE (Amarsi) · [1], [2], [8], [9], [10] Si-products-5b8d060cc69b

NIR · Kitt Peak (Kurucz 2005) · Si I · Codex-graded lines · 1D LTE · [1], [2], [9], [6] Si-products-64e9c7ec5eff

NIR · Kitt Peak (Kurucz 2005) · Si I · Codex-graded lines · 1D NLTE (Amarsi) · [1], [2], [9], [10] Si-products-a9deb819e9d6

NIR · Kitt Peak (1984, molecfit) · Si I · Deshmukh et al. 2022 lines · 1D LTE · [1], [2], [11], [9], [6] Si-products-1cf235ed25e2

NIR · Kitt Peak (1984, molecfit) · Si I · Deshmukh et al. 2022 lines · 1D NLTE (Amarsi) · [1], [2], [11], [9], [10] Si-products-8f73eeee5ec7

NIR · Kitt Peak (1984, molecfit) · Si I · Elgueta et al. 2026 lines · 1D LTE · [1], [2], [8], [9], [6] Si-products-87cc2c806d35

NIR · Kitt Peak (1984, molecfit) · Si I · Elgueta et al. 2026 lines · 1D NLTE (Amarsi) · [1], [2], [8], [9], [10] Si-products-9ce6d851e54f

NIR · Kitt Peak (1984, molecfit) · Si I · Codex-graded lines · 1D LTE · [1], [2], [9], [6] Si-products-917519bb8b08

NIR · Kitt Peak (1984, molecfit) · Si I · Codex-graded lines · 1D NLTE (Amarsi) · [1], [2], [9], [10] Si-products-d3e7a2d5806c

NIR · Kitt Peak (1984, molecfit) · Si I · reference lines · 1D LTE · [1], [2], [9], [6] Si-products-26c33238276a

NIR · Kitt Peak (1984, molecfit) · Si I · reference lines · 1D NLTE (Amarsi) · [1], [2], [9], [10] Si-products-f40b7f18aec7

VIS · HARPS · Si I · Asplund et al. 2021 lines · 1D LTE · [1], [2], [3], [4], [5], [6] Si-products-399d79152258

VIS · HARPS · Si I · Asplund et al. 2021 lines · 3D NLTE (Amarsi) · [1], [2], [3], [4], [5] Si-products-e56a754ec56c

VIS · HARPS · Si I · Asplund et al. 2021 lines · 1D NLTE (Amarsi) · [1], [2], [3], [4], [5], [10] Si-products-ba2021480936

VIS · HARPS · Si I · Codex-graded lines · 1D LTE · [1], [2], [3], [4], [5], [6] Si-products-c00d8a68c882

VIS · HARPS · Si I · Codex-graded lines · 3D NLTE (Amarsi) · [1], [2], [3], [4], [5] Si-products-8e0dd07f6984

VIS · HARPS · Si I · Codex-graded lines · 1D NLTE (Amarsi) · [1], [2], [3], [4], [5], [10] Si-products-9d2425feeb2a

VIS · HARPS · Si I · reference lines · 1D LTE · [1], [2], [3], [4], [5], [6] Si-products-44d8adf7b692

VIS · HARPS · Si I · reference lines · 3D NLTE (Amarsi) · [1], [2], [3], [4], [5] Si-products-5724d945e6b8

VIS · HARPS · Si I · reference lines · 1D NLTE (Amarsi) · [1], [2], [3], [4], [5], [10] Si-products-32fad1920f54

VIS · Kitt Peak (Kurucz 2005) · Si I · Asplund et al. 2021 lines · 1D LTE · [1], [2], [3], [4], [5], [6] Si-products-86963d196c1b

VIS · Kitt Peak (Kurucz 2005) · Si I · Asplund et al. 2021 lines · 3D NLTE (Amarsi) · [1], [2], [3], [4], [5] Si-products-b240a324cc32

VIS · Kitt Peak (Kurucz 2005) · Si I · Asplund et al. 2021 lines · 1D NLTE (Amarsi) · [1], [2], [3], [4], [5], [10] Si-products-7fc64a528c54

VIS · Kitt Peak (Kurucz 2005) · Si I · Codex-graded lines · 1D LTE · [1], [2], [3], [4], [5], [6] Si-products-329cbcbeac77

VIS · Kitt Peak (Kurucz 2005) · Si I · Codex-graded lines · 3D NLTE (Amarsi) · [1], [2], [3], [4], [5] Si-products-99784bfdea9f

VIS · Kitt Peak (Kurucz 2005) · Si I · Codex-graded lines · 1D NLTE (Amarsi) · [1], [2], [3], [4], [5], [10] Si-products-404ec2791d1e

VIS · Kitt Peak (Kurucz 2005) · Si I · reference lines · 1D LTE · [1], [2], [3], [4], [5], [6] Si-products-00341643fead

VIS · Kitt Peak (Kurucz 2005) · Si I · reference lines · 3D NLTE (Amarsi) · [1], [2], [3], [4], [5] Si-products-4b3dba1395ae

VIS · Kitt Peak (Kurucz 2005) · Si I · reference lines · 1D NLTE (Amarsi) · [1], [2], [3], [4], [5], [10] Si-products-e43dd39e0d59

VIS · Kitt Peak (1984, molecfit) · Si I · Asplund et al. 2021 lines · 1D LTE · [1], [2], [3], [4], [5], [6] Si-products-39dc00c1a14f

VIS · Kitt Peak (1984, molecfit) · Si I · Asplund et al. 2021 lines · 3D NLTE (Amarsi) · [1], [2], [3], [4], [5] Si-products-cd8bc6507892

VIS · Kitt Peak (1984, molecfit) · Si I · Asplund et al. 2021 lines · 1D NLTE (Amarsi) · [1], [2], [3], [4], [5], [10] Si-products-c7a79094da61

VIS · Kitt Peak (1984, molecfit) · Si I · Codex-graded lines · 1D LTE · [1], [2], [3], [4], [5], [6] Si-products-06bc587092cd

VIS · Kitt Peak (1984, molecfit) · Si I · Codex-graded lines · 3D NLTE (Amarsi) · [1], [2], [3], [4], [5] Si-products-3763b5ead261

VIS · Kitt Peak (1984, molecfit) · Si I · Codex-graded lines · 1D NLTE (Amarsi) · [1], [2], [3], [4], [5], [10] Si-products-8f16da367055

VIS · Kitt Peak (1984, molecfit) · Si I · reference lines · 1D LTE · [1], [2], [3], [4], [5], [6] Si-products-a8bae74e1637

VIS · Kitt Peak (1984, molecfit) · Si I · reference lines · 3D NLTE (Amarsi) · [1], [2], [3], [4], [5] Si-products-e90f2ed95209

VIS · Kitt Peak (1984, molecfit) · Si I · reference lines · 1D NLTE (Amarsi) · [1], [2], [3], [4], [5], [10] Si-products-79251de431b4

red-optical · IAG FTS · Si I · Asplund et al. 2021 lines · 1D LTE · [1], [2], [3], [4], [5], [6] Si-products-b657c77ce6c1

red-optical · IAG FTS · Si I · Asplund et al. 2021 lines · 3D NLTE (Amarsi) · [1], [2], [3], [4], [5] Si-products-97cb84e08024

red-optical · IAG FTS · Si I · Asplund et al. 2021 lines · 1D NLTE (Amarsi) · [1], [2], [3], [4], [5], [10] Si-products-a7cd9505fdba

red-optical · IAG FTS · Si I · Codex-graded lines · 1D LTE · [1], [2], [3], [4], [5], [7], [9], [6] Si-products-d073ae2a2257

red-optical · IAG FTS · Si I · Codex-graded lines · 3D NLTE (Amarsi) · [1], [2], [3], [4], [5] Si-products-09760af0cf60

red-optical · IAG FTS · Si I · Codex-graded lines · 1D NLTE (Amarsi) · [1], [2], [3], [4], [5], [7], [9], [10] Si-products-3d989c66efeb

red-optical · IAG FTS · Si I · reference lines · 1D LTE · [1], [2], [3], [4], [5], [6] Si-products-6dbf4752431e

red-optical · IAG FTS · Si I · reference lines · 3D NLTE (Amarsi) · [1], [2], [3], [4], [5] Si-products-65d308abd42b

red-optical · IAG FTS · Si I · reference lines · 1D NLTE (Amarsi) · [1], [2], [3], [4], [5], [10] Si-products-eb98a2ca787c

red-optical · Kitt Peak (Kurucz 2005) · Si I · Asplund et al. 2021 lines · 1D LTE · [1], [2], [3], [4], [5], [6] Si-products-c0f52cd2b939

red-optical · Kitt Peak (Kurucz 2005) · Si I · Asplund et al. 2021 lines · 3D NLTE (Amarsi) · [1], [2], [3], [4], [5] Si-products-e2d52b23cce2

red-optical · Kitt Peak (Kurucz 2005) · Si I · Asplund et al. 2021 lines · 1D NLTE (Amarsi) · [1], [2], [3], [4], [5], [10] Si-products-e6d971e0b94c

red-optical · Kitt Peak (Kurucz 2005) · Si I · Codex-graded lines · 1D LTE · [1], [2], [3], [4], [5], [7], [9], [6] Si-products-0f3e0551bc3d

red-optical · Kitt Peak (Kurucz 2005) · Si I · Codex-graded lines · 3D NLTE (Amarsi) · [1], [2], [3], [4], [5] Si-products-570a2042f74e

red-optical · Kitt Peak (Kurucz 2005) · Si I · Codex-graded lines · 1D NLTE (Amarsi) · [1], [2], [3], [4], [5], [7], [9], [10] Si-products-7ffe29671e4d

red-optical · Kitt Peak (Kurucz 2005) · Si I · reference lines · 1D LTE · [1], [2], [3], [4], [5], [6] Si-products-f12901402645

red-optical · Kitt Peak (Kurucz 2005) · Si I · reference lines · 3D NLTE (Amarsi) · [1], [2], [3], [4], [5] Si-products-475cbc839e72

red-optical · Kitt Peak (Kurucz 2005) · Si I · reference lines · 1D NLTE (Amarsi) · [1], [2], [3], [4], [5], [10] Si-products-24e55c1ecea5

red-optical · Kitt Peak (1984, molecfit) · Si I · Asplund et al. 2021 lines · 1D LTE · [1], [2], [3], [4], [5], [6] Si-products-91cdd1cf5623

red-optical · Kitt Peak (1984, molecfit) · Si I · Asplund et al. 2021 lines · 3D NLTE (Amarsi) · [1], [2], [3], [4], [5] Si-products-76551597a1d6

red-optical · Kitt Peak (1984, molecfit) · Si I · Asplund et al. 2021 lines · 1D NLTE (Amarsi) · [1], [2], [3], [4], [5], [10] Si-products-288b8030736c

red-optical · Kitt Peak (1984, molecfit) · Si I · Codex-graded lines · 1D LTE · [1], [2], [3], [4], [5], [7], [9], [6] Si-products-11510ddc4eb0

red-optical · Kitt Peak (1984, molecfit) · Si I · Codex-graded lines · 3D NLTE (Amarsi) · [1], [2], [3], [4], [5] Si-products-af09e5e283d3

red-optical · Kitt Peak (1984, molecfit) · Si I · Codex-graded lines · 1D NLTE (Amarsi) · [1], [2], [3], [4], [5], [7], [9], [10] Si-products-886285c645ec

red-optical · Kitt Peak (1984, molecfit) · Si I · reference lines · 1D LTE · [1], [2], [3], [4], [5], [6] Si-products-b1d5d2332406

red-optical · Kitt Peak (1984, molecfit) · Si I · reference lines · 3D NLTE (Amarsi) · [1], [2], [3], [4], [5] Si-products-88d3364eaa70

red-optical · Kitt Peak (1984, molecfit) · Si I · reference lines · 1D NLTE (Amarsi) · [1], [2], [3], [4], [5], [10] Si-products-99115adc8bd8

NIR · CRIRES+ Y (full arm) · Si I · Elgueta et al. 2026 lines · 1D NLTE (Amarsi) · [1], [2], [8], [9], [10] Si-quarantine-d49aee5458f3

NIR · CRIRES+ J · Si I · Elgueta et al. 2026 lines · 1D NLTE (Amarsi) · [1], [2], [8], [9], [10] Si-quarantine-cc2f7729c860

Complete applicable bibliography

Solar abundance and indicator analyses

[1] — Asplund, M.; Amarsi, A. M.; Grevesse, N. (2021). The chemical make-up of the Sun: A 2020 vision. A&A 653, A141 DOI: 10.1051/0004-6361/202140445. source record

[2] — Lodders, K.; Bergemann, M.; Palme, H. (2025). Solar System Elemental Abundances from the Solar Photosphere and CI-Chondrites. Space Science Reviews 221 DOI: 10.1007/s11214-025-01146-w. source record

[3] — Amarsi, A. M.; Asplund, M. (2017). The solar silicon abundance based on 3D non-LTE calculations. MNRAS 464, 264-273 DOI: 10.1093/mnras/stw2445. source record

[8] — Elgueta, S.; Jofre, P.; Aguilera-Gomez, C.; Slumstrup, D.; Rojas Arriagada, A.; Heiter, U.; Casamiquela, L.; Zoccali, M.; Worley, C.; Soubiran, C. (2026). Gaia FGK benchmark stars: Selecting infrared lines for abundance determination. A&A 710, A111 DOI: 10.1051/0004-6361/202659148. source record

[11] — Deshmukh, S. A.; Ludwig, H.-G.; Kucinskas, A.; et al. (2022). The solar photospheric silicon abundance according to CO5BOLD: Investigating line broadening, magnetic fields, and model effects. A&A 668, A48 DOI: 10.1051/0004-6361/202142072. source record

Atomic data and gf authorities

[4] — Garz, T. (1973). Absolute oscillator strengths of Si I lines between 2500 A and 8000 A. A&A 26, 471-477 source record

[5] — O'Brian, T. R.; Wickliffe, M. E.; Lawler, J. E.; Whaling, W.; Brault, J. W. (1991). Lifetimes, transition probabilities, and level energies in Fe I. JOSA B 8, 1185 DOI: 10.1364/JOSAB.8.001185. source record

[7] — Kelleher, D. E.; Podobedova, L. I. (2008). Atomic Transition Probabilities of Silicon. A Critical Compilation. J. Phys. Chem. Ref. Data 37, 1285-1501 DOI: 10.1063/1.2734566. source record

[9] — Pehlivan Rhodin, A.; Hartman, H.; Nilsson, H.; Joensson, P. (2024). Accurate and experimentally validated transition data for Si I and Si II. A&A 682, A184 DOI: 10.1051/0004-6361/202245686. source record

Model and grid sources

[6] — Gerber, J. M.; Magg, E.; Plez, B.; Bergemann, M.; Heiter, U.; Olander, T.; Hoppe, R. (2023). Non-LTE radiative transfer with Turbospectrum. A&A 669, A43 DOI: 10.1051/0004-6361/202243673. source record

[10] — Amarsi, A. M.; Lind, K.; Osorio, Y.; Nordlander, T.; Bergemann, M.; et al. (2020). The GALAH Survey: non-LTE departure coefficients for large spectroscopic surveys. A&A 642, A62 DOI: 10.1051/0004-6361/202038650. source record